

# Effects of Prehafnizing on Morphological Development of a Chemical Vapor Deposition Aluminide Coating Formed on Single-Crystal Ni-Based Superalloy

L.M. HE, J.D. MEYER, and W.Y. LEE

We examined a sequential Hf doping procedure, which consisted of (1) “prehafnizing” the surface of a single-crystal Ni-based superalloy (RENÉ N5) with  $\text{HfCl}_4$  and  $\text{H}_2$ , and (2) aluminizing with  $\text{AlCl}_3$  and  $\text{H}_2$ , as a means of incorporating Hf as a dopant in the aluminide coating matrix. The prehafnized layer on RENÉ N5 substrate significantly altered the growth behavior and therefore the morphology of the resulting aluminide coating. With the prehafnizing step, the coating layer became much thinner with a significant amount of Hf incorporated as Hf-rich phases ( $\text{Hf}_2\text{Ni}_7$ ,  $\text{Hf}_3\text{Ni}_7$ , and/or  $\text{Hf}_8\text{Ni}_{21}$ ). However, the Hf-rich phases segregated to the coating surface and retarded the inward Al diffusion required to form the  $\beta$ -NiAl coating matrix. The sequential Hf doping procedure provided a mechanism to incorporate a significant amount of Hf in the coating, but did not produce a uniform distribution of Hf as a dopant. The results were compared to those observed for a continuous doping procedure that was previously studied, and were discussed in the context of understanding the limitations of these procedures.

## I. INTRODUCTION

RECENT manufacturing advances in aluminizing by chemical vapor deposition (CVD) offer new processing opportunities to improve significantly the performance of single-phase  $\beta$ -NiAl and (Ni,Pt)Al bond coatings for next-generation thermal barrier coating applications.<sup>[1–3]</sup> The  $\beta$ -NiAl and  $\beta$ -(Ni,Pt)Al coatings produced on a single-crystal Ni alloy by the “low-activity” CVD process<sup>[2,3,4]</sup> typically exhibit a columnar coating microstructure characterized by a two-dimensional network of grain boundaries with the formation of ridges at the intersection between the coating surface and the grain boundaries.

As previously reported,<sup>[5]</sup> we have studied the morphological development of the aluminide coating matrix at the early stages of aluminizing. After 5 minutes of aluminizing at 1150 °C,  $\gamma$ -Ni<sub>3</sub>Al particles of ~100-nm diameter randomly nucleated on the alloy surface. As shown in Figure 1,<sup>[5]</sup> within 20 minutes, a coating layer consisting of preferentially oriented, columnar  $\beta$ -NiAl grains was formed with the segregation of refractory elements (*i.e.*, Ta and W) from the alloy to coating grain boundaries. The grain boundaries originated at the substrate surface, and extended to the coating surface. The formation of a diffusion zone was also observed underneath the coating layer. Precipitates were enriched with refractory alloying elements due to the outward diffusion of Ni from the alloy during formation of the external aluminide layer.

As previously elaborated,<sup>[6]</sup> the dynamic versatility of the CVD aluminizing process provides a potential avenue to uniformly dope the coating matrix with a reactive element (*e.g.*, Hf) *via* proactive control of the gas-phase concentration

of the dopant precursor ( $\text{HfCl}_4$ ) as a function of time. The beneficial effects of reactive elements such as Hf, Y, and Zr on the oxidation performance of Ni-based superalloys and coating materials have been well documented.<sup>[7–13]</sup> In this study, we examined a sequential Hf doping procedure, which consisted of (1) “prehafnizing” the alloy surface with  $\text{HfCl}_4$  and  $\text{H}_2$ , and (2) sequentially aluminizing with  $\text{AlCl}_3$  and  $\text{H}_2$ . Our major objectives were to (1) determine the effects of the prehafnizing procedure on the morphological development of the subsequent aluminide coating matrix and the distribution of Hf in the coating matrix and (2) compare the effectiveness of the sequential procedure to that of the continuous procedure that was previously studied.<sup>14</sup>

## II. EXPERIMENTAL

A single-crystal Ni superalloy (RENÉ N5)\* was cast as

\*RENÉ N5 is a trademark of General Electric Company, Fairfield, CT.

a cylindrical rod with a [100] seed orientation. The alloy rod was sliced radially to produce disc specimens (0.2-cm thickness and 1.2-cm diameter) while preserving the [100] orientation on the disc surface. The nominal composition (in wt pct) of the alloy is 6.2Al, 0.05C, 7.5Co, 7.0Cr, 0.16Hf, 1.5Mo, 3.0Re, 6.5Ta, 0.02Ti, 5.0W, with Ni as the balance. The alloy was melt-desulfurized to below 1 ppm sulfur by PCC Airfoils. Also, a long polycrystalline Ni (99.99 pct, purity) strip (10 × 1 × 0.5 cm) was used as a model substrate for comparison.

A laboratory-scale, hot-wall CVD reactor was used to perform sequential Hf doping experiments. The schematics and major features of the reactor were previously described elsewhere.<sup>[14,15]</sup> The procedure for the sequential Hf doping experiments started with evacuation of the reactor and sample loading chamber to ~13 Pa. The reactor chamber was then heated to 1150 °C ( $\pm 5$  °C) while flowing  $\text{H}_2$  at a reactor pressure of 13.3 kPa. Once the desired temperature was

L.M. HE, formerly Postdoctoral Candidate, Department of Chemical, Biochemical and Materials Engineering, Stevens Institute of Technology, Hoboken, NJ 07030, is with the Georgia Institute of Technology, Atlanta, GA. J.D. MEYER, Postdoctoral Candidate, and W.Y. LEE, Professor, are with the Department of Chemical, Biochemical and Materials Engineering, Stevens Institute of Technology. Contact e-mail: wlee@stevens-tech.edu  
Manuscript submitted October 2, 2002.

reached,  $\text{HfCl}_4$  was added to start the prehafnizing step. The flow rate of  $\text{H}_2$  (99.999 pct purity) was  $300 \text{ cm}^3/\text{min}$  at STP, while the flow rate of  $\text{HCl}$  used to chlorinate Hf pellets (99.95 pct purity) was  $50 \text{ cm}^3/\text{min}$ . After 0.5 min of prehafnizing, the  $\text{HfCl}_4$  and  $\text{H}_2$  flows were stopped, and the reactor chamber was evacuated to remove all residual gas species in the chamber. After the evacuation step, the reactor pressure was returned to 13.3 kPa by introducing  $\text{H}_2$  and then  $\text{AlCl}_3$  to start the aluminizing step.

For the aluminizing step, the flow rate of  $\text{H}_2$  was  $300 \text{ cm}^3/\text{min}$ , and that of  $\text{HCl}$  used to chlorinate Al pellets (99.9 pct purity) was  $50 \text{ cm}^3/\text{min}$ . After 20 minutes of aluminizing, the  $\text{AlCl}_3$  and  $\text{H}_2$  flows were stopped, the reactor was evacuated, and the substrates were retrieved from the hot reactor. The retrieval of the substrates took several minutes, during which the cooling rate of the substrate was about  $\sim 200 \text{ }^\circ\text{C}/\text{min}$ . This experimental procedure was repeated for the prehafnizing time of 5, 10, and 30 minutes, while

the aluminizing time was held constant at 20 minutes. Also, two additional experiments were performed to hafnize RENÉ N5 and Ni substrates for 10 minutes without the subsequent aluminizing step. Table I summarized the coating samples generated from these experiments in terms of processing parameter variations. For example, 10Hf-20Al-N5 denotes that the coating sample was formed after (1) 10 minutes prehafnizing and (2) 20 minutes subsequent aluminizing on a RENÉ N5 substrate.

The coated substrates were cross sectioned metallographically, and an etchant ( $5\text{HCl}$  and  $1\text{HNO}_3$ ) was used to expose morphological features. A scanning electron microscope (SEM) equipped with an energy-dispersive spectrometer (EDS) was used for microstructure and qualitative compositional evaluation. An X-ray diffractometer (XRD) was used for phase determination. The elemental compositions of some coating specimens were analyzed as a function of coating depth by glow discharge mass spectrometry (GDMS). The

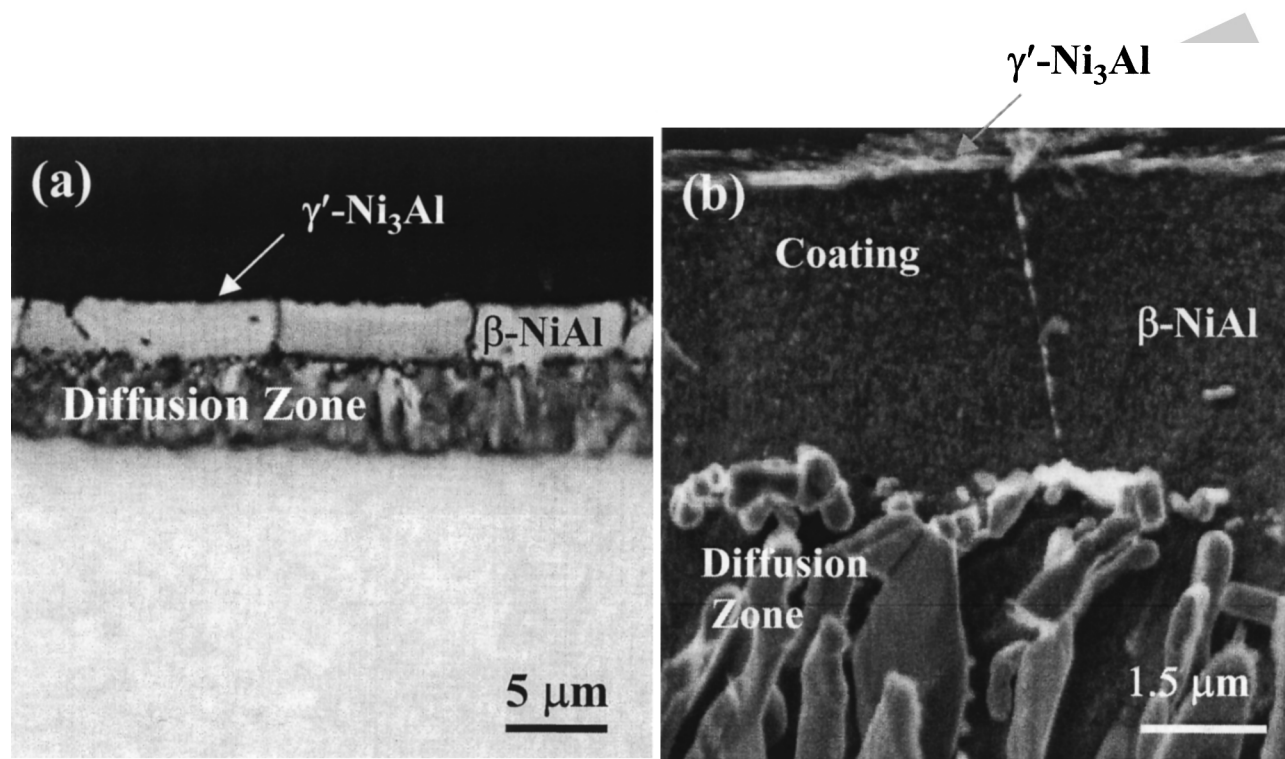


Fig. 1—(a) and (b) SEM cross-sectional images for 20Al-N5.<sup>[5]</sup>

**Table I. Summary of Observed Microstructural Changes**

Sample Number	20Al-N5	0.5Hf-20Al-N5	5Hf-20Al-N5	10Hf-20Al-N5	10Hf-20Al-Ni	20Al-Ni
Substrate	RENÉ N5	RENÉ N5	RENÉ N5	RENÉ N5	pure Ni	pure Ni
Prehafnizing time (min)	0	0.5	5	10	10	0
Aluminizing time (min)	20	20	20	20	20	20
Average grain diameter* ( $\mu\text{m}$ )	$\sim 7.5$	—	$\sim 1.5$	$\sim 1.8$	$\sim 20$	$\sim 25$
Coating thickness** ( $\mu\text{m}$ )	$\sim 3.6$	$\sim 3.8$	$\sim 2.0$	$\sim 1.7$	$\sim 10.7$	$\sim 12$
Diffusion zone thickness ( $\mu\text{m}$ )	$\sim 5.7$	—	—	—	—	—
Aspect ratio <sup>†</sup>	$\sim 2.1$	—	—	—	$\sim 1.9$	$\sim 2.1$

\*Determined from surface micrographs by the mean grain intercept method.<sup>[13]</sup>

\*\*Determined from cross-sectional micrographs.

<sup>†</sup>Aspect ratio = average grain diameter/coating thickness.

procedures developed for GDMS calibration, normalization, and data analyses are described elsewhere.<sup>[16]</sup>

### III. RESULTS

As shown in Figure 2(a), even with 0.5-minutes prehafnizing (0.5Hf-20Al-N5), coating morphology was significantly changed from that of the pure aluminide coating (20Al-N5) shown in Figure 1. The thickness of the coating layer with the prehafnizing step ( $\sim 3.8 \mu\text{m}$ ) was much thinner than that of the pure aluminizing coating ( $\sim 9.3 \mu\text{m}$ , including the coating layer and the diffusion zone). Underneath the coating layer, the presence of a distinct diffusion zone was not clearly observed. However, the  $\gamma/\gamma'$  network structure of the superalloy underneath the coating layer became somewhat irregular and distorted, as its typical square shape was elongated in the direction parallel to the

coating/alloy interface. Also, the  $\gamma'$  phase in this region appeared to grow in size.

From the cross-sectional images (Figures 2(b) and (c)) of the coating samples with 5 and 10 minutes of prehafnizing (5Hf-20Al-N5 and 10Hf-20Al-N5), the thicknesses of the two coatings were measured to be similar ( $\sim 2 \mu\text{m}$ ), but both were thinner than the sample with 0.5 minutes of prehafnizing ( $\sim 3.8 \mu\text{m}$ ). Underneath the coating layer, a diffusion zone was not observed on either sample. The  $\gamma'$  precipitates in the  $\gamma/\gamma'$  alloy structure were elongated and enlarged from their original square shape for the two samples, as observed for the 0.5-minutes sample.

An XRD pattern obtained for the 10-minutes prehafnizing coating (10Hf-20Al-N5, Figure 3(a)) indicated that the coating layer consisted of  $\beta$ -NiAl as a major phase and minor amounts of  $\text{Hf}_3\text{Ni}_7$ ,  $\text{Hf}_8\text{Ni}_{21}$ , and/or  $\gamma'$ -Ni<sub>3</sub>Al. As shown in Figure 2(d), a thin high-contrast ( $\sim 0.3\text{-}\mu\text{m}$ -thick) layer was observed on the surface of the 10-minutes prehafnizing

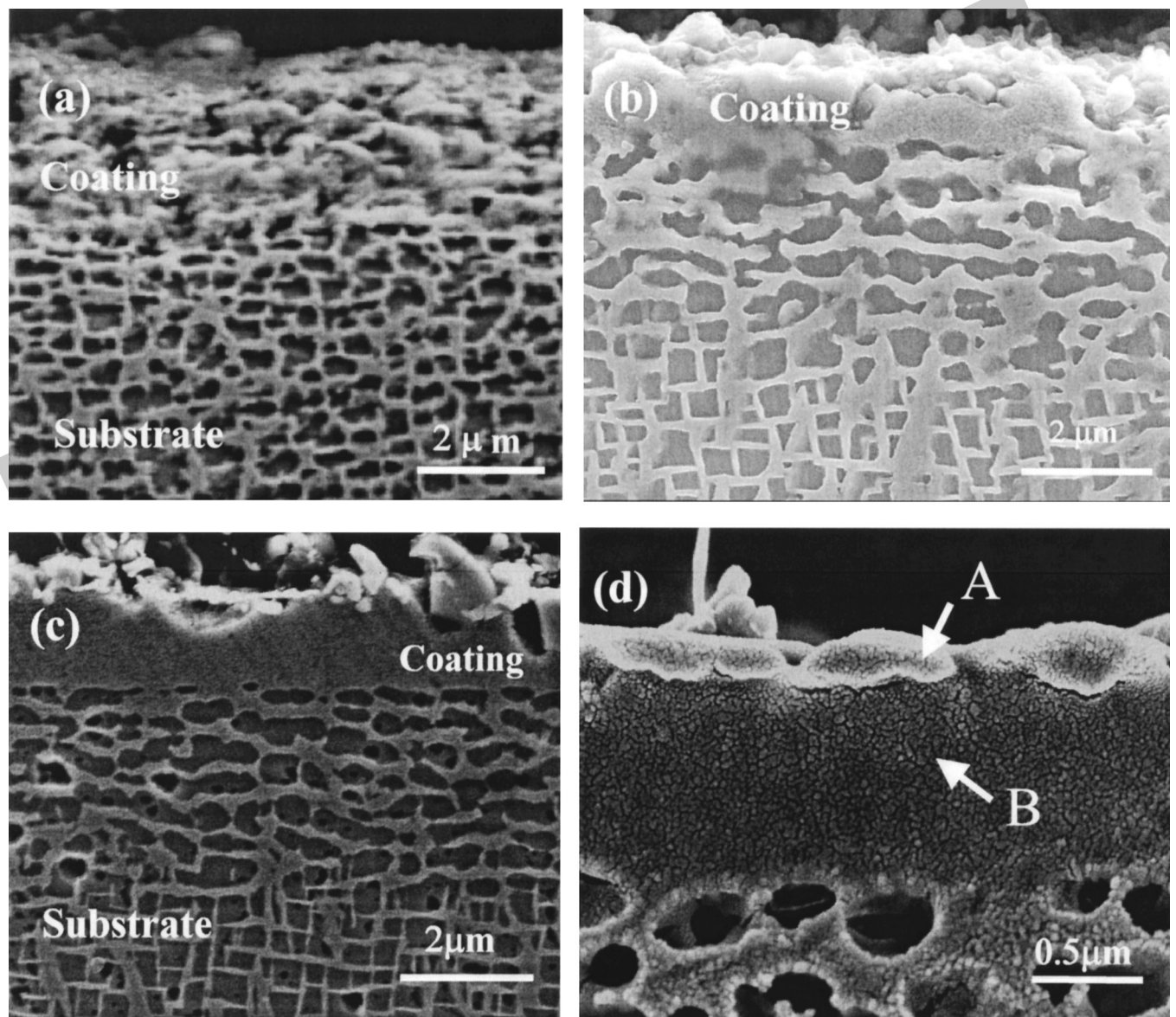


Fig. 2—SEM cross-sectional images of (a) 0.5Hf-20Al-N5, (b) 5Hf-20Al-N5, and (c) and (d) 10Hf-20Al-N5.

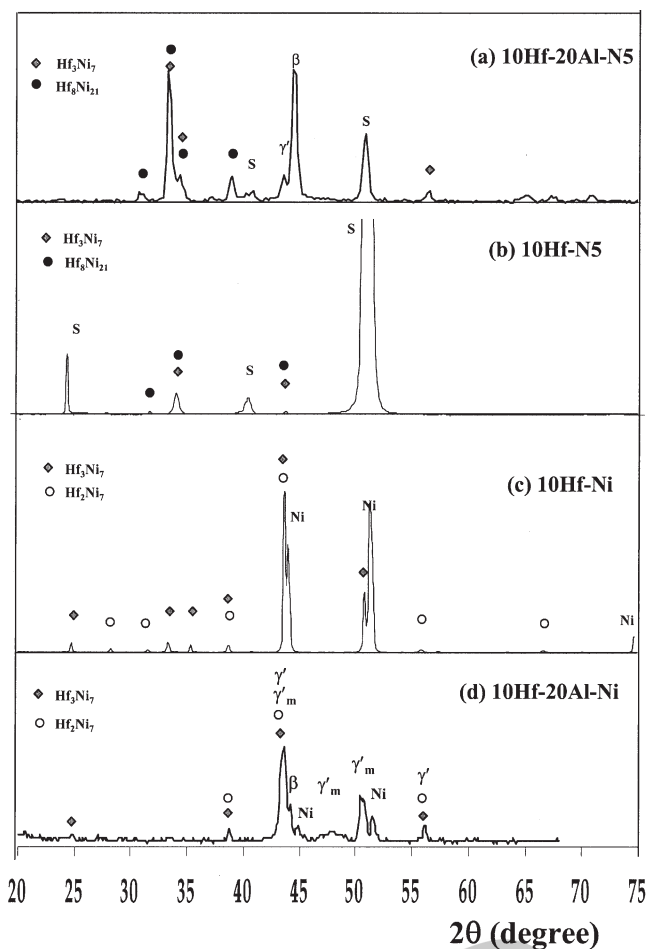


Fig. 3—(a) through (d) XRD patterns.

coating. The thin layer was continuous, and fully covered the coating surface. The EDS analysis shown in Figure 4(a) suggested that the thin layer contained Hf as a dominant element and small amounts of Cr, Co, Al, and Ni. The EDS analysis of the coating matrix underneath this thin layer, as shown in Figure 4(b), indicated that Ni, Al, Cr, and Hf concentrations were high. These EDS/SEM observations suggested that Hf segregated to the coating surface.

The coating sample produced after 10 minutes of hafnizing (*i.e.*, without further aluminizing, 10Hf-N5) on the Ni-based superalloy substrate was also characterized. As shown in Figure 5(a), the coating surface consisted of small grains in the range of  $\sim 50$  to  $\sim 300$  nm. From the cross-sectional SEM/EDS analysis, as summarized in Figure 3(b), the coating consisted of two layers: (1)  $\sim 200$ -nm-thick Hf-rich layer at the surface and (2)  $\sim 1$ - $\mu\text{m}$ -thick interlayer in which the Hf concentration appeared to be lower than that in the top layer. As shown in Figure 3(b), XRD data indicated that the coating layer consisted of a  $\text{Hf}_8\text{Ni}_{21}$  and/or  $\text{Hf}_3\text{Ni}_7$  phases.

The coating formed after 10 minutes of hafnizing without aluminizing (10Hf-Ni) on a pure Ni substrate revealed a different coating morphology from the coating formed on the Ni-based superalloy substrate (10Hf-N5). As shown in Figure 6, the coating was  $\sim 2$ - $\mu\text{m}$  thick with relatively large grain size ( $\sim 4$   $\mu\text{m}$ ). The presence of small discrete areas ( $\sim 200$  to  $\sim 500$  nm), which appeared as “dark” in the surface micro-

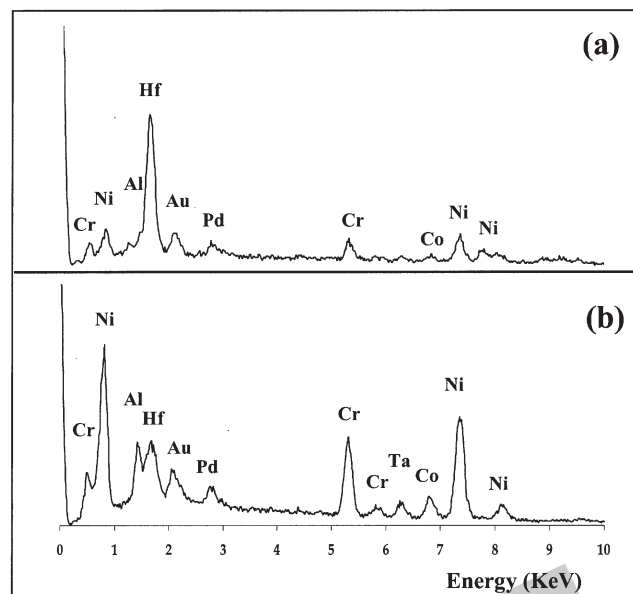


Fig. 4—EDS spectra from (a) location A and (b) location B in Fig. 2(d) (10Hf-20Al-N5). Note that the Pd and Au peaks are from the SEM sample preparation procedure.

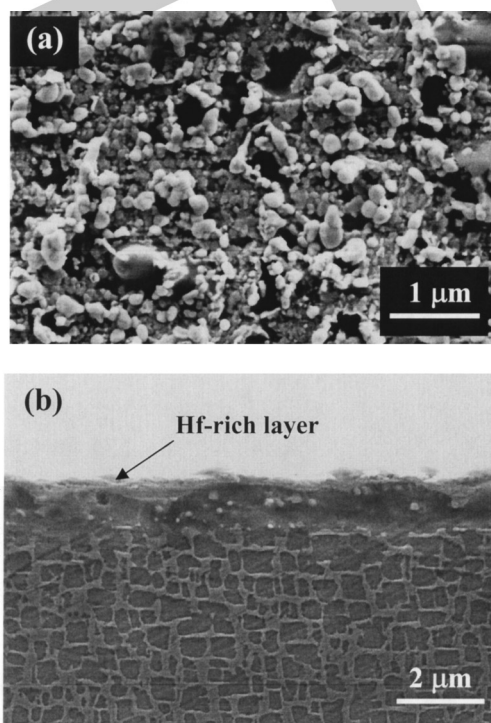


Fig. 5—SEM images of 10Hf-N5: (a) surface and (b) cross section.

graph, was observed. Also, a thin continuous layer ( $\sim 500$ -nm thick) was observed at the coating surface, but this layer could not be compositionally resolved with the EDS analysis. The XRD pattern of the 10Hf-Ni coating, as shown in Figure 3(c), indicated that the coating consisted of  $\text{Hf}_2\text{Ni}_7$  and/or  $\text{Hf}_3\text{Ni}_7$  phases. In comparison of the XRD peak intensities of  $\text{Hf}_2\text{Ni}_7$  and  $\text{Hf}_3\text{Ni}_7$  to those of powder diffraction patterns in the database, we indexed the  $\text{Hf}_2\text{Ni}_7$  phase as a minor phase. Note

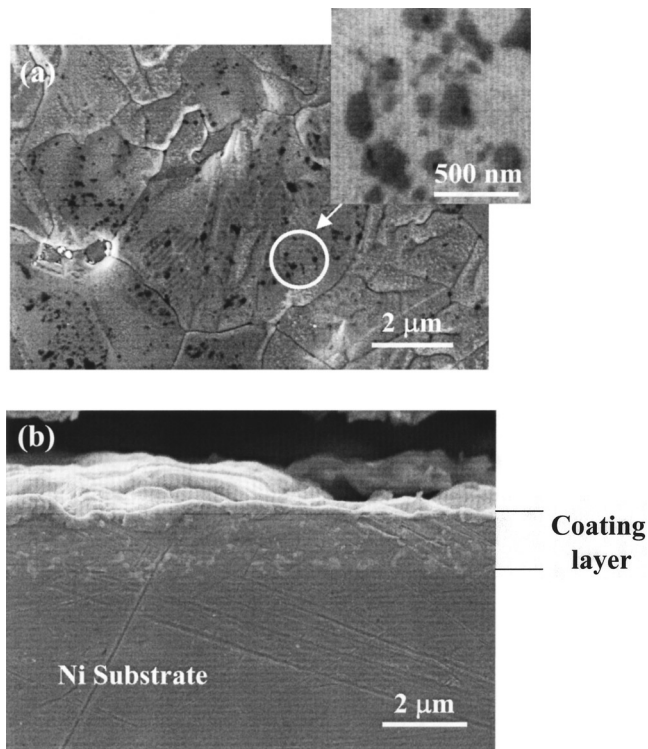


Fig. 6—SEM images of 10Hf-Ni: (a) surface and (b) cross section.

that  $\text{Hf}_2\text{Ni}_7$  has a monoclinic crystal structure, whereas  $\text{Hf}_3\text{Ni}_7$  and  $\text{Hf}_8\text{Ni}_{21}$  have triclinic structures.

Figure 7(a) shows the cross-sectional SEM image of the coating formed with 10 minutes of prehafnizing and 20 minutes of aluminizing on pure Ni substrate (10Hf-20Al-Ni). The coating had two distinct regions: (1) an inner layer of  $\sim 5 \mu\text{m}$  with elongated precipitates at the coating/substrate interface and (2) a uniform outer layer of  $\sim 5 \mu\text{m}$ . The outer coating layer had a columnar coating microstructure with an average grain diameter of  $\sim 20 \mu\text{m}$ . In comparison, the coating formed on a pure Ni substrate by 20 minutes of aluminizing without prehafnizing (20Al-Ni) demonstrated a similar columnar coating morphology, which was observed *via* our cross-sectional SEM images (not shown in this article). This coating (20Al-Ni) contained large grains ( $\sim 25 \mu\text{m}$ ) and was thick ( $\sim 12 \mu\text{m}$ ), as tabulated in Table I.

In Figure 7(b), the GDMS depth profiling of the 10Hf-20Al-Ni coating suggested that the inner layer contained high Hf concentrations (up to a peak concentration of  $\sim 4$  wt pct), whereas the Al concentration decreased continually through this layer. In the outer layer, the Al concentration was  $\sim 21$  wt pct while that of Ni was  $\sim 78$  wt pct. The Hf concentration in this region was 0.08 wt pct, and showed uniform distribution except for the sharp rise to 0.7 wt pct at the coating surface.

The XRD pattern of 10Hf-20Al-Ni shown in Figure 3(d) suggested that the coating contained  $\gamma'$ ,  $\gamma'_m$  (a martensitic phase of  $\gamma'$ ),  $\beta$ ,  $\text{Hf}_2\text{Ni}_7$ , and  $\text{Hf}_3\text{Ni}_7$  phases in the coating layer. The SEM image (Figure 7(a)) shows the presence of a typical platelike martensitic microstructure in the outer coating layer. The martensitic phase apparently resulted from  $\beta$

to  $\gamma'_m$  phase transformation due to the high Ni concentration of the NiAl phase during rapid sample cooling in our CVD process.<sup>[14]</sup>

#### IV. DISCUSSION

The Hf concentration in the coating layer formed on RENÉ N5 with the prehafnizing time of 0.5 to 10 minutes was high. The high concentration was attributed to the presence of Hf-rich phases ( $\text{Hf}_2\text{Ni}_7$ ,  $\text{Hf}_3\text{Ni}_7$ , and/or  $\text{Hf}_8\text{Ni}_{21}$ ) in the layers. Also, the Hf-rich phases apparently coexisted with  $\beta$ -NiAl and  $\gamma'$ -Ni<sub>3</sub>Al phases in the coating layer, but appeared to be segregated to the coating surface (Figure 4). As discussed elsewhere,<sup>[14]</sup> the solubility limits of Hf in  $\beta$ -NiAl and  $\gamma'$ -Ni<sub>3</sub>Al have not been explicitly measured or reported in the literature. However, the limit was estimated to be  $\sim 0.2$  wt pct for stoichiometric cast NiAl.<sup>[10]</sup> We note that the coating specimens did not contain the Heusler phase ( $\text{Ni}_2\text{AlHf}$ ), which is known to be one of the phases commonly observed in the Ni-Al-Hf system.<sup>[17,18,19]</sup>

The microstructure of the aluminide coating formed after 20 minutes of aluminizing, without prehafnizing, was distinctively columnar, as shown in Figure 1. However, with prehafnizing, development of the columnar microstructure was not observed. Even for the prehafnizing time of only 0.5 minutes, the coating morphology deviated significantly (Figure 2(a)). Furthermore, the vertical growth behavior of the coating layer was also significantly affected by the prehafnizing step. For example, the thickness of the aluminide coating without prehafnizing was  $\sim 9.3 \mu\text{m}$  (Figure 1), whereas that of the coating obtained with the 10-minute prehafnizing step followed by 20 minutes of aluminizing was less than  $\sim 2 \mu\text{m}$  (Figure 2(c)). The average grain diameter, as measured using SEM surface micrographs, decreased from  $\sim 7.5$  to  $\sim 1.8 \mu\text{m}$  with 10 minutes of prehafnizing (Table I).

Without prehafnizing, the presence of a well-established diffusion zone with precipitates of refractory elements was clear evidence for the outward diffusion of Ni atoms from the alloy surface to the coating layer.<sup>[5]</sup> However, neither a characteristic diffusion zone nor precipitates of refractory elements was observed underneath the coating layer for all the coating samples prepared on RENÉ N5 substrate with prehafnizing regardless of the duration of the prehafnizing time. The result suggested that the outward diffusion of Ni required for reaction with  $\text{AlCl}_3$  at the coating surface was retarded by a diffusion barrier effect of the prehafnized alloy surface.

A thin layer ( $\sim 0.3\text{-}\mu\text{m}$ -thick) was observed at the coating surface of 10 minutes prehafnizing sample (10Hf-20Al-N5) along with significant Hf segregation (Figures 2(d) and 4). This Hf-rich layer appeared to be responsible for the diffusion barrier effect. As explained in our previous study,<sup>[14]</sup> the formation of the thin  $\gamma'$ -Ni<sub>3</sub>Al layer observed at the surface of the aluminide coating (Figure 1) formed on RENÉ N5 was promoted by the enrichment of refractory alloying elements at the coating surface. Furthermore, our previous results also suggested that the growth of the  $\beta$ -NiAl layer actually occurred at the  $\gamma'$ -Ni<sub>3</sub>Al/ $\beta$ -NiAl interface and consequently the  $\gamma'$ -Ni<sub>3</sub>Al phase appeared to “float” at the coating surface during aluminizing. This growth behavior was believed to be caused by (1) the diffusion of Al being faster



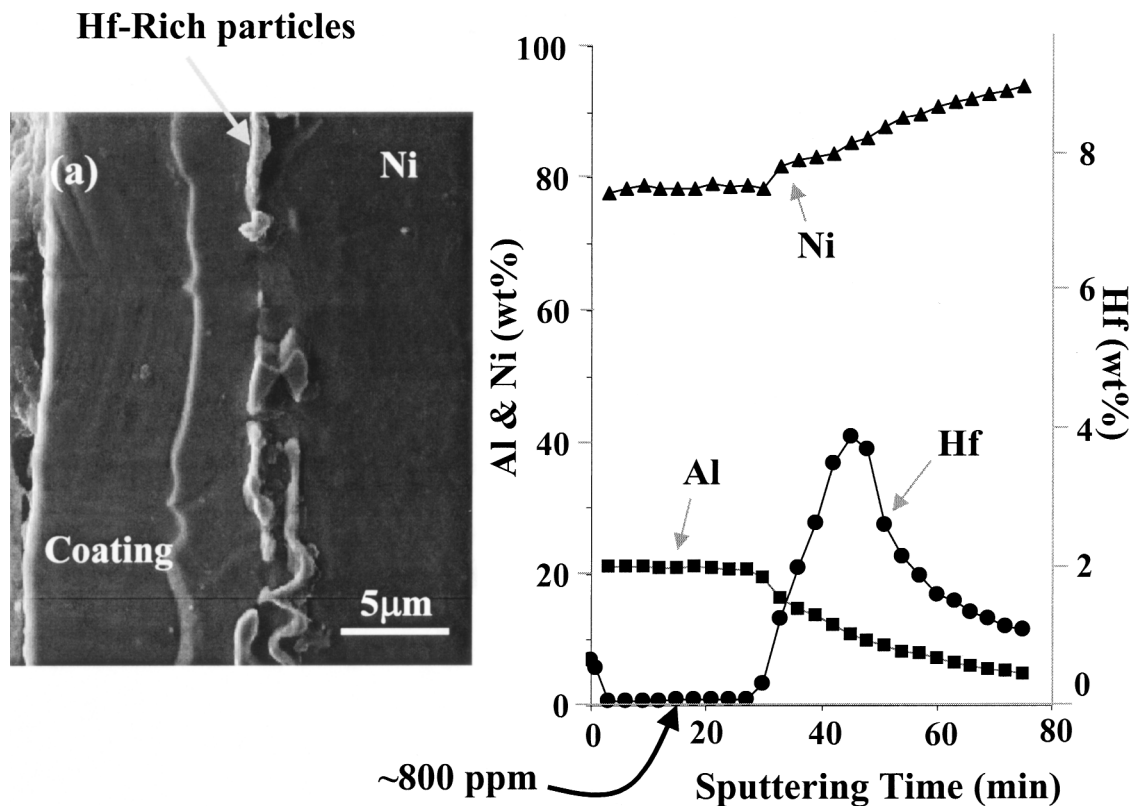


Fig. 7—Microstructure and composition of 10Hf-20Al-Ni: (a) cross-sectional SEM and (b) GDMS depth profiles.

than that of Ni through the Al-rich  $\gamma'$ -Ni<sub>3</sub>Al layer and (2) the diffusion of Ni being faster than that of Al through the Ni-rich  $\beta$ -NiAl layer.<sup>[14]</sup> It is possible that the Hf-rich layer might have reduced the rate of Al inward diffusion, thus working as a diffusion barrier.

With a very short prehafnizing step (*e.g.*, 0.5 minutes), it appeared that a thinner Hf-rich layer was formed. The thinner Hf-rich layer might have allowed some Al diffusion, and resulted in the retarded  $\beta$ -NiAl growth shown in Figure 2(a). With increased prehafnizing time, the Hf-rich layer could have become thick enough. In this case, the further growth of  $\beta$ -NiAl beneath the Hf-rich layer was significantly retarded.

As mentioned previously, the  $\gamma/\gamma'$  network structure of Ni-based superalloy underneath the coating layer was distorted and elongated, while  $\gamma$  phase in this region grew in size (Figure 2(c)). As reported by Pichior,<sup>[20]</sup> in the aluminizing process, the loss of Ni in the alloy resulted in the transformation of the  $\gamma/\gamma'$  network structure to the  $\beta$ -NiAl phase with the precipitates enriched with refractory elements. The diffusion barrier effect therefore was responsible in this incomplete  $\gamma/\gamma'$  to  $\beta$  transformation and the distortion of the  $\gamma/\gamma'$  network structure.

On a pure Ni substrate, the effect of the prehafnizing step on the coating morphology structure was less notable than on the Ni-based superalloy. The columnar structure was retained in the prehafnized coating, as shown in Figure 7(a). The prehafnizing coating contained somewhat smaller grains ( $\sim 20 \mu\text{m}$ ) vs the coating without prehafnizing ( $\sim 25 \mu\text{m}$ ), while its coating thickness became slightly thinner ( $\sim 11$  vs  $\sim 12 \mu\text{m}$ ).

The embedding of the Hf-rich phases in the inner layer of the coating (Figure 7(a)) indicated that the coating growth interface was most likely above the Hf-rich layer. A possible reason for this behavior could be related to reactions between the Ni substrate and the Ni-Hf phases. As the Ni substrate reacts with the Hf-Ni phases, the prehafnized layer might become discontinuous (Figure 7(a)). Consequently, the diffusion barrier effect of the hafnized layer would be diminished.

Our results show that the sequential Hf doping procedure certainly provides a mechanism to incorporate a significant amount of Hf in the coating, but it did not produce uniform Hf distribution on RENÉ N5. Furthermore, the segregation of the Hf-rich precipitates to the surface significantly retarded the growth of the  $\beta$ -NiAl coating matrix and adversely affected the development of columnar coating morphology. In contrast, the amount of Hf incorporated into the coating matrix by a continuous doping procedure, as described elsewhere in detail<sup>[14,15]</sup> and as briefly summarized earlier, was lower than the intended concentration range ( $\sim 0.1$  to 1.2 wt pct).

The continuous doping procedure, in which HfCl<sub>4</sub> and AlCl<sub>3</sub> were simultaneously introduced with H<sub>2</sub>, produced a very low Hf content in the  $\beta$ -NiAl layer ( $\sim 0.01$  wt pct) at relatively low HfCl<sub>4</sub>/AlCl<sub>3</sub> ratios. Also, the Hf incorporated into the coating layer was mainly from the substrate. The apparent solubility of Hf in the  $\beta$ -NiAl aluminide coating layer formed on RENÉ N5 was significantly lower ( $\sim 0.01$  wt pct) than that observed for pure stoichiometric NiAl ( $\sim 0.2$  wt pct) due to the partitioning of other refractory elements such as Ta into the coating layer. In this interpretation, Hf and the other refractory elements are expected to

compete for the same Al sublattice sites in the NiAl coating layer. When the HfCl<sub>4</sub> concentration in the gas phase was increased, the average Hf content in the coating layer increased to ~0.1 wt pct. But, the increase was attributed to the formation of Hf-rich precipitates primarily at grain boundaries in the coating matrix.

The sequential and continuous procedures represented the two extreme cases in terms of controlling Hf doping time as a process parameter, and therefore the results from the procedures provided an important basis for understanding the limitations of the procedures and designing time-resolved Hf doping approaches. For example, 0.5 minutes of prehafnizing resulted in what appeared to be a very thin layer of Hf-rich layer at the coating surface, and therefore the diffusion barrier effect became less apparent. We expect that the diffusion barrier effect could further be lessened if the prehafnizing time were to be much less than 0.5 minutes and if accompanied by a number of small hafnizing intervals during the course of the overall aluminizing process. Such a procedure modification may eliminate the observed diffusion barrier effect while uniformly incorporating Hf in the  $\beta$ -NiAl coating matrix.

## V. CONCLUSIONS

We examined a sequential Hf doping procedure, which consisted of (1) prehafnizing the surface of a single-crystal Ni-based superalloy (RENE N5) with HfCl<sub>4</sub> and H<sub>2</sub>, and (2) sequentially aluminizing with AlCl<sub>3</sub> and H<sub>2</sub>, as a means of incorporating Hf as a dopant in the aluminide coating matrix. Our major objectives were to (1) determine the effects of the prehafnizing procedure on morphological development of the subsequent coating matrix and the distribution of Hf in the coating matrix and (2) compare the effectiveness of the sequential procedure to that of a continuous procedure that has been previously studied. The prehafnized layer on RENÉ N5 substrate significantly altered the growth behavior and therefore the morphology of the resulting aluminide coating. With the prehafnizing step, the coating layer became much thinner with a significant amount of Hf incorporated as Hf-rich phases (Hf<sub>2</sub>Ni<sub>7</sub>, Hf<sub>3</sub>Ni<sub>7</sub>, and/or Hf<sub>8</sub>Ni<sub>21</sub>). However, the Hf-rich phases segregated to the coating surface, and retarded the Al inward diffusion required to form the  $\beta$ -NiAl coating matrix. Therefore, the sequential Hf doping procedure provided a mechanism to incorporate a significant amount of Hf in the coating, but did not produce a uniform distribution of Hf as a dopant.

The sequential and continuous procedures represented the two extreme cases in terms of controlling Hf doping time as a process parameter, and therefore the results from the procedures provided an important basis for understanding the limitations of the procedures and designing time-resolved Hf doping approaches. The diffusion barrier effect could further be lessened if the prehafnizing time were to be much less than 0.5 minutes and if accompanied by a number of

small hafnizing intervals during the course of the overall aluminizing process. Such a procedure modification might eliminate the diffusion barrier effect observed while incorporating Hf in the  $\beta$ -NiAl coating matrix.

## ACKNOWLEDGMENTS

This research was sponsored by the National Science Foundation (Contract No. DMR9801042) and Advanced Gas Turbine System Program, United States Department of Energy Office of Industrial Technologies, under Contract No. DE-AC05-96OR22464, with Lockheed Martin Energy Research Corporation. One of the author (JDM) was supported, in part, by the Robert C. Stanley Fellowship. We also acknowledge contributions to this work by J.A. Haynes, Oak Ridge National Laboratory; R. Darolia, General Electric Aircraft Engines; and K. Putyera, Shiva Technologies.

## REFERENCES

1. B. Nagaraj: U.S. Patent 5,427,866, 1995.
2. W.Y. Lee, Y. Zhang, I.G. Wright, B.A. Pint, and P.K. Liaw: *Metall. Mater. Trans. A*, 1998, vol. 29A, pp. 833-41.
3. Y. Zhang, W.Y. Lee, J.A. Haynes, I.G. Wright, B.A. Pint, K.M. Cooley, and P.K. Liaw: *Metall. Mater. Trans. A*, 1999, vol. 30A, pp. 2679-687.
4. J.A. Haynes, Y. Zhang, W.Y. Lee, B.A. Pint, I.G. Wright, and K.M. Cooley: in *Elevated Temperature Coatings: Science and Technology III*, J.M. Hampikian and N.B. Dahotre, eds., TMS, Warrendale, PA, 1999, pp. 185-96.
5. G.Y. Kim, W.Y. Lee, J.A. Haynes, and T.R. Watkins: *Metall. Mater. Trans. A*, 2001, vol. 32A, pp. 615-24.
6. W.Y. Lee and G.Y. Kim: in *Elevated Temperature Coatings: Science and Technology III*, J.M. Hampikian and N.B. Dahotre, eds., TMS, Warrendale, PA, 1999, pp. 149-60.
7. A.W. Funkenbusch, J.G. Smeggil, and N.S. Bornstein: *Metall. Trans. A*, 1985, vol. 16A, pp. 1164-66.
8. D.K. Gupta: U.S. Patent 4,933,329, 1990.
9. B.A. Pint: *Oxid. Met.*, 1996, vol. 45, pp. 1-37.
10. B.A. Pint, I.G. Wright, W.Y. Lee, Y. Zhang, K. Prüßner, and K.B. Alexander: *Mater. Sci. Eng.*, 1998, vol. A245, pp. 201-11.
11. R. Bianco and R.A. Rapp: *J. Electrochem. Soc.*, 1993, vol. 140, pp. 1181-90.
12. D.C. Tu, C.C. Lin, S.J. Liao, and J.C. Chou: *J. Vac. Sci. Technol.*, 1986, vol. A4, pp. 2601-06.
13. R. Prescott and M.J. Graham: *Oxid. Met.*, 1992, vol. 38 (3-4), pp. 233-54.
14. G.Y. Kim, L.M. He, J.D. Meyer, A. Quintero, and W.Y. Lee: *Metall. Mater. Trans. A*, 2003, vol. 34A, pp. 0000-00.
15. G.Y. Kim, L.M. He, J.D. Meyer, and W.Y. Lee: in *Surface Engineering in Materials Science I*, S. Seal, N.B. Dahotre, J.J. Moore, and B. Mishra, eds., TMS, Warrendale, PA, 2000, pp. 69-78.
16. L.M. He, K. Putyera, J.D. Meyer, L.R. Walker, and W.Y. Lee: *Metall. Mater. Trans. A*, 2003, vol. 34A, pp. 0000-00.
17. J.D. Whittenberger, I.E. Locci, R. Darolia, and R. Bowman: *Mater. Sci. Eng.*, 1999, vol. A268, pp. 165-83.
18. K. Oh-ishi, Z. Horita, and M. Nemeto: *Mater. Sci. Eng.*, 1997, vols. A239-240, pp. 472-78.
19. I.E. Locci, R.M. Dickerson, A. Garg, R.D. Noebe, J.D. Whittenberger, M.V. Nathal, and R. Darolia: *J. Mater. Res.*, 1996, vol. 11, pp. 3024-38.
20. R. Pichoir: in *Materials and Coatings to Resist High Temperature Corrosion*, D.R. Holmes and A. Rahmel, eds., Applied Science Publishers Ltd., London, 1978, pp. 271-91.



# Summary of Comments on 02-502A-11.qxd

---

## Page: 1

---

Sequence number: 1

Author: dames

Date: 11/7/2003 1:16:16 AM

Type: Note

Author: Please provide present title of position and department at Georgia Tech for author He. Please provide a zip code for Georgia Tech.

Sequence number: 2

Author: dames

Date: 11/7/2003 1:17:04 AM

Type: Note

Author: Please provide name and city and state or country location for vendor of PCC Airfoils.

## Page: 5

---

Sequence number: 1

Author: dames

Date: 11/7/2003 1:17:54 AM

Type: Note

Author: Are the changes to the indicated sentence okay?

## Page: 6

---

Sequence number: 1

Author: dames

Date: 11/7/2003 1:18:51 AM

Type: Note

Author: Are the changes to the indicated sentence okay?

## Page: 7

---

Sequence number: 1

Author: dames

Date: 11/7/2003 1:19:25 AM

Type: Note

Author: Reference 20: Is the publisher's name correct?



## Online Proofing Guidance Page

### **FIRST STEP:**

Install Adobe Acrobat Reader if you do not already have this or another Acrobat product installed on your computer. You can do this free of charge by connecting to the Adobe site and following the instructions at:

<http://www.adobe.com/products/acrobat/readermain.html>

### **SECOND STEP:**

Please download and print your PDF file — we recommend that you save this file to disk, rather than opening it from within your Browser.

#### **From a PC:**

1. Right-click on the file/article link.
2. Select “Save Target as”
3. Select a desired location on your computer to save the file to, and click on “Save”
4. Open your PDF file directly with Acrobat Reader or another Acrobat product.
5. Print this file as you normally would with any typical application. Example: Go up to your toolbar, select “File”, select “Print”.

#### **From a MAC:**

1. Hold the mouse button down over the link.
  - a. In Internet Explorer, select “Download Link to Disk” from the resulting pop-up menu
  - b. In Netscape, select “Save this Link as” from the resulting pop-up menu
2. Select a desired location on your computer and click on “Save”
3. Open your PDF file directly with Acrobat Reader or another Acrobat product.
4. Print this file as you normally would with any typical application. Example: Go up to your menu bar, select “File”, select “Print”.

### **THIRD STEP:**

Please go through the file you have just printed and thoroughly and clearly mark any revisions you would like to see implemented in your paper. If you have had any changes in phone/fax or e-mail addresses since your paper was submitted, please send us this new information.

### **FOURTH STEP:**

#### **Your revised paper needs to be faxed or mailed to:**

IPC Print Services  
Attn: Sheryl Dickenson  
501 Colonial Drive  
St. Joseph, MI 49085  
Fax number: 1-269-983-4064

#### **If you have questions regarding your paper in general, you may email or telephone:**

IPC Print Services  
Attn: Sheryl Dickenson  
Email: [sdickens@ipcjci.com](mailto:sdickens@ipcjci.com)  
Phone: 1-269-983-7412, ext. 529